Psychophysical definition of S-cone stimuli in the macaque

Nathan Hall

Department of Neuroscience and Center for the Neural Basis of Cognition, University of Pittsburgh, Pittsburgh, PA, USA

Carol Colby

Department of Neuroscience and Center for the Neural Basis of Cognition, University of Pittsburgh, Pittsburgh, PA, USA

We used the perceptual reports of nonhuman primates to perform psychophysical calibrations of S-cone isolating stimuli. S-cone stimuli were calibrated separately at several spatial locations for each monkey. To do this we exploited the effect of transient tritanopia, which causes a selective decrease of sensitivity in the observer's S-cone channel. At the start of each transient tritanopia trial monkeys were visually adapted to a bright yellow background. This type of adaptation is known to induce transient tritanopia. Calibrated S-cone isolating stimuli were determined by finding a near S-cone stimulus whose detection threshold was maximally elevated during transient tritanopia. At the start of each control trial, monkeys were adapted to a bright white background. In these trials, monkeys' detection thresholds for near S-cone stimuli were unchanged. We found that S-cone isolating stimuli could be determined at most locations tested in each monkey. Calibrated S-cone stimuli were particular to both spatial location and animal. To understand the visual system as a whole in vivo requires physiological methods not possible in human subjects. The present results open the door to novel behavioral and physiological experiments by showing that S-cone isolating stimuli can be calibrated in monkeys.

Introduction

The S-cone system

In vision experiments it is often desirable to isolate specific visual processing subsystems. Creating a stimulus that can do this is not straightforward and typically requires a subject-specific psychophysical calibration. Psychophysical calibrations must be based on perceptual experience—something that is easy to ascertain in human subjects via verbal report. Our goal here was to use the nonverbal perceptual report of monkeys to perform psychophysical calibrations similar to those done in human subjects. The procedure developed allows us to create a stimulus that isolates excitation to a specific cone subsystem.

Photopic vision in old world primates is driven by the activation of three classes of cone receptors in the retina. Blue cones, or S-cones, are those most sensitive to the short wavelengths of visible light. The S-cone system differs from other visual subsystems in a number of important ways. The S-cone system is phylogenetically older (Yokoyama & Yokoyama, 1989) and in many ways peculiar compared to long (L) and middle (M) wavelength sensitive cone systems (Calkins, 2001). For example, S-cone signals are carried by their own slowly conducting class of retinal ganglion cell (Dacey & Lee, 1994). Such differences in the processing of S-cone input have made the study of this subsystem the focus of numerous investigations. Stimuli calibrated by the procedure described here can be used to study S-cone systems physiologically by selectively altering excitation of S-cones in macaque monkeys.

S-cone isolating stimuli in humans

Stimuli that selectively activate S-cones (or S-cone isolating stimuli) can be used to study the S-cone system. These stimuli cause no change in L- and M-cone excitation. A true S-cone isolating stimulus differs from one based solely on cone sensitivity spectra mainly because of macular pigment in the eye (Sumner, Adamjee, & Mollon, 2002). Macular pigment selectively absorbs short-wavelength blue light (Snodderly, Brown, Delori, & Auran, 1984b) where S-cones are most sensitive. The amount of macular pigment absorption depends on the viewer and even varies by retinal location within individuals. These factors make it

Citation: Hall, N., & Colby, C. (2013). Psychophysical definition of S-cone stimuli in the macaque. *Journal of Vision*, *13*(2):20, 1–18, http://www.journalofvision.org/content/13/2/20, doi:10.1167/13.2.20.

doi: 10.1167/13.2.20 Received July 10, 2012; published February 14, 2013 ISSN 1534-7362

difficult to construct an S-cone isolating stimulus. S-cone isolating stimuli must be calibrated for individual observers and spatial locations. This requires a calibration procedure to identify S-cone isolating stimuli at desired experimental locations for each subject.

Several studies have adopted a calibration procedure to determine S-cone isolating stimuli. These calibration procedures have all been performed on human subjects and are based on the procedure proposed by Smithson, Sumner, and Mollon (2003). Armed with S-cone isolating stimuli for each individual subject and test location, researchers have investigated a variety of questions about the function of the S-cone system. Behavioral analyses using S-cone isolating stimuli have shown that the S-cone system is slower than other visual systems (Smithson & Mollon, 2004), especially within oculomotor networks (Bompas & Sumner, 2008). In particular, the role of the superior colliculus (SC) has been studied using S-cone stimuli, to which the SC is believed to be blind (de Monasterio, 1978; Schiller, Malpeli, & Schein, 1979; Sumner et al., 2002). These investigations have probed the role of the SC in oculomotor behavior (Sumner et al., 2002; Sumner, Nachev, Vora, Husain, & Kennard, 2004; Sumner, Nachev, Castor-Perry, Isenman, & Kennard, 2006; A. J. Anderson & Carpenter, 2008) and clinically in studies of blindsight and interhemispheric transfer (Savazzi & Marzi, 2004; Leh, Mullen, & Ptito, 2006; Savazzi et al., 2007; Leh, Ptito, Schönwiesner, Chakravarty, & Mullen, 2010). These studies of human subjects all share the common theme of isolating brain structures by using S-cone isolating stimuli.

S-cone isolating stimuli in nonhuman primates

All studies using calibrated S-cone isolating stimuli to date have been performed on human subjects. The use of animal models allows the collection of neurophysiological as well as behavioral data. Macaque monkeys are excellent models of trichromatic cone mediated vision. Macaque color vision and perception are nearly identical to that of humans as found both psychophysically via behavioral report (De Valois, Morgan, Polson, Mead, & Hull, 1974; Huang, MacEvoy, & Paradiso, 2002) and physiologically by studying the spectral sensitivity of the three cone types (Bowmaker, Dartnall, Lythgoe, & Mollon, 1978; Bowmaker & Dartnall, 1980). The distribution of retinal S-cones is likewise similar in both species, being most numerous around the fovea and forming a semiregular distribution more eccentrically (Curcio, Sloan, Packer, Hendrickson, & Kalina, 1987; Bumsted & Hendrickson, 1999). Both humans and monkeys have macular pigment that is most dense near the fovea and decreases toward the periphery (Snodderly, Auran, & Delori, 1984a; Snodderly et al., 1984b; Trieschmann et al., 2007). The spatial extent of macular pigment varies between individuals. This variation has lead researchers using psychophysical studies in humans to calibrate S-cone isolating stimuli for each subject and each spatial location used experimentally. Similarities between humans and monkeys in visual processing make it both possible and necessary to calibrate S-cone isolating stimuli in macaques using procedures like those used in humans.

Our goal was to determine S-cone isolating stimuli in macaque monkeys. Our methods are conceptually similar to those Smithson et al. (2003) proposed for use on human subjects. The similarity between the two procedures provides a critical bridge between previous human psychophysics studies and future work in monkeys using S-cone isolating visual stimuli. We found that it is possible to calibrate S-cone isolating stimuli in macaque monkeys. The colors of these stimuli are similar to those found for humans and likewise depend on the individual observer and spatial location tested.

Methods

Subjects and data acquisition

Two adult male rhesus monkeys (*Macaca mulatta*) were used in these experiments. Animals were cared for and handled in accordance with National Institutes of Health guidelines. The University of Pittsburgh Institutional Animal Care and Use Committee approved all experimental protocols. Monkeys weighed 13 and 8.5 kg (monkey CA and monkey FS, respectively). Both had normal trichromatic color vision as evidenced by their ability to distinguish L-cone isolating stimuli (data not shown) in addition to their ability to resolve S-cone isolating stimuli. During experiments, animals sat in a primate chair with head fixed. Monkeys viewed a CRT monitor at a distance of 30 cm. Eye position was monitored using scleral search coils (Judge, Richmond, & Chu, 1980) with a Riverbend field driver and signal processing filter (Riverbend Technologies Inc.). Eye position voltages were continuously monitored online through NIMH Cortex software (provided by Dr. Robert Desimone) and saved for offline analysis on a separate computer running Plexon software (Plexon Inc.). Offline analysis was carried out on custom MATLAB® (Mathworks, Natick, MA) software that detected saccades, trial events, and trial outcomes.

Stimulus presentation and control

Stimulus timing and presentation were controlled using NIMH Cortex software. Stimuli were presented

on a computer controlled 19-inch ViewSonic® color CRT monitor at a refresh rate of 85 Hz using an 8-bit DAC with an ATI Radeon™ X600 SE graphics card. To generate stimuli, the monitor was calibrated for color and luminance using a Photo Research PR-655 SpectraScan® spectroradiometer integrated with custom MATLAB® (Mathworks, Natick, MA) software. Actual stimuli used were verified for accuracy in both color and luminance using the same setup. Colors for stimuli were chosen from MacLeod-Boynton (MB) color space (MacLeod & Boynton, 1979) as defined using the Smith and Pokorny cone fundamentals (Smith & Pokorny, 1975). We modified MB space such that the vertical axis represents relative S-cone excitation times four, as has been done previously (Smithson et al., 2003). Color coordinates in this paper refer to this modified MB color space which we will simply call MB space.

Experimental approach

Our approach takes advantage of "transient tritanopia" (Mollon & Polden, 1975) in a manner first proposed by Smithson et al. (2003). The principle is that sensitivity in the S-cone opponent channel is briefly and selectively decreased after adaptation to a bright yellow background. In other words, there is a transient blindness to activation of the third, "tritan" cone (or S-cone) channel, i.e., tritanopia. Elevated L- and M-cone channel activity persists after excessive stimulation by the bright yellow background resulting in selective suppression of S-cone opponent pathways. S-cone channel activity must outweigh that of L- and M-cones in order to detect increased S-cone contrast. Elevated L- and M-cone activation means that greater S-cone excitation is needed to outweigh them and thus detect an S-cone stimulus—i.e. S-cone detection threshold is increased. The increase in threshold will be greatest for a stimulus that best matches the exact S-cone isolation point for a given viewer.

The objective of experimental calibration was to determine S-cone isolating stimuli separately for each monkey at six spatial locations. An S-cone isolating stimulus will always lie along a tritan confusion line. A tritan line is a line in color space representing a series of colors that are distinguishable only on the basis of S-cone stimulation. Colors along a tritan line represent constant levels of excitation in L- and M-cones, while excitation for S-cones varies. All colors along a subject's tritan confusion line would be perceived as identical were their S-cones suddenly removed. Such a tritan line lies in an equiluminant plane in MB color space.

The equiluminant MB plane (~20.7 cd/m^2) from which our stimuli were chosen is shown in Figure 1. Because the spectral sensitivity of the three classes of retinal cones overlaps, an S-cone isolating stimulus, and thus a tritan line, must be determined with respect to a background color. The background and stimulus colors are chosen so that their degrees of L- and M-cone excitations are equal. We used the standard equal energy gray (EEG) point (0.667, 0.060) as our background color. Radiating outward from this point are candidate tritan vectors. Candidate vectors are used to find the actual tritan line and are chosen to be near the theoretical tritan line. The vertical vector represents the theoretical tritan line through EEG in MB space. The bright adapting backgrounds (luminance 53.5 cd/m^2) used were either white (0.651, 0.048) or yellow (0.664, 0.004).

Task design

At the start of each trial, a fixation cross was presented on an EEG background and the monkey had 200 ms to acquire fixation (Figure 2). During fixation, the background changed to one of two possible adapting states. During control trials, the background was bright white. During tritanopia trials the background was bright yellow to induce transient tritanopia. The monkey then fixated for 7600 ms to allow for adequate adaption. This fixation period is much longer than in many primate oculomotor tasks. To encourage monkeys to maintain fixation on this bright background, one drop of liquid reward was delivered after 3000 ms and again after 6000 ms of fixation. Control trials place an upper bound on detection thresholds in the absence of transient tritanopia. They demonstrate that detection thresholds do not change across candidate tritan vectors at contrasts above 0.018 from EEG. Thresholds are lower in this case because there is no selective desensitization of S-cone channels, i.e., a lack of transient tritanopia. Control and tritanopia trials were run in separate sessions.

After adaptation, the fixation cross was extinguished and simultaneously a 1° × 1° stimulus target square appeared. This square represented both the test stimulus color and the saccade target. This stimulus target was embedded in a full screen background array of 1° × 1° gray squares (Figure 2). The square was presented in one of six possible locations randomly chosen on each trial at 4° eccentricity for monkey FS and 6° for monkey CA. Six screen locations were tested for each animal because the identity of the true tritan vector varies by location as well as individual. During a given ~2 hour daily session monkeys performed approximately 140–240 trials. Both animals typically performed more trials during the easier control compared to tritanopia sessions. In each session stimulus target colors were chosen from a single

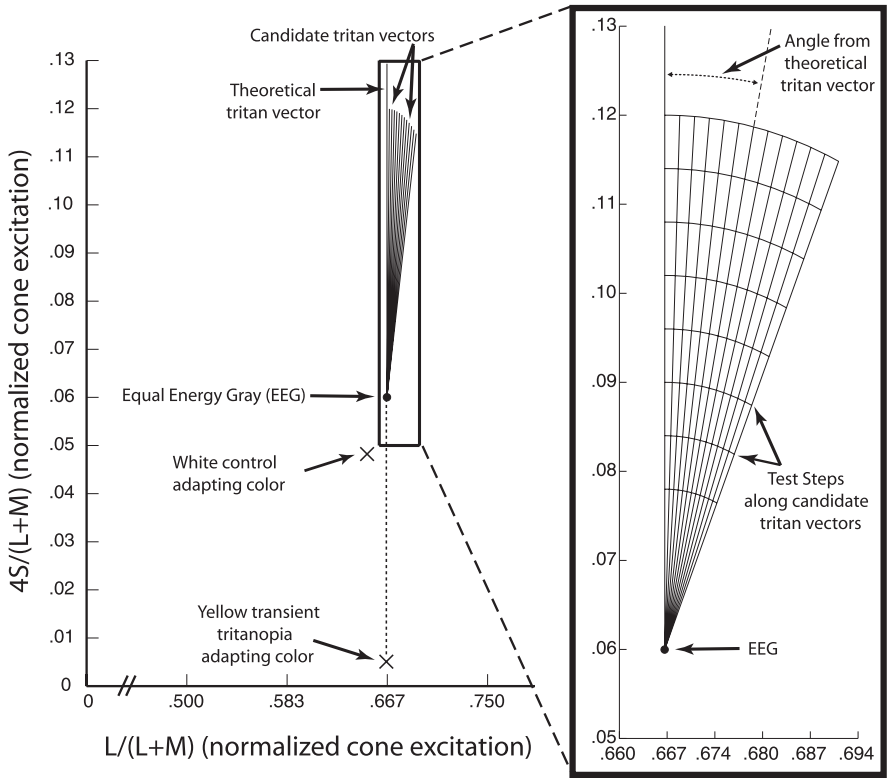

Figure 1. Scaled MacLeod-Boynton space. The main figure shows the version of MacLeod-Boynton (MB) space used for determining stimulus and background colors. This MB space is scaled so that values for S-cone excitation on the vertical axis are multiplied by four to give similar control performance across candidate tritan vectors following the procedure of Smithson et al. (2003). The horizontal axis is truncated as no points outside of those shown were used. EEG (filled circle) was the background color for experiments. The theoretical (vertical) and candidate (angled) tritan vectors tested are shown as lines in the equiluminant plane radiating from EEG. Xs indicate the color coordinates of the adapting backgrounds but signify that they do not lie in the equiluminant plane of the tritan vectors. Adapting backgrounds were much brighter than the plane shown and therefore lie above it along the *z*-axis rising out of the page. The expanded view on the right details vectors and test steps. Candidate vectors were chosen and labeled as angles from the theoretical line (0° to 24°). Curves running across tritan vectors mark the eight test steps. Test steps were increments of 0.006 units in the scaled MB space starting at 0.018 units and measured as distance from EEG along each vector. Points in MB space used to find detection thresholds lay at the points of intersection between the vectors and test steps.

candidate tritan vector. Stimulus target color was chosen randomly on each trial. The color was one of eight possible test steps, representing distance from EEG and chosen to be at the intersection of one of the test step curves with a candidate tritan vector (Figure 1). Luminance of the stimulus target square matched the median luminance of background squares (approximately 20.7 cd/m^2). All background squares were of the same color (EEG) but their individual luminances were randomly selected on each trial. Individual background squares took one of nine possible luminance values at intervals spaced approximately 0.5 cd/m^2 apart with range 18.8 to 22.6 cd/m^2. The background array of gray squares served to mask luminance artifacts so that the stimulus target square could be detected only on the basis of chromatic contrast (Birch, Barbur, & Harlow, 1992; Sumner et al., 2002). Background squares were positioned so that the stimulus target square was aligned into the background grid. The display of stimulus target and background squares was presented for approximately 24 ms for monkey CA and 106 ms for monkey FS. Target presentation time was adjusted until detection of the lowest S-cone contrast test step stimulus was near chance (1/6) or well below our 50% detection threshold for each monkey. This was determined during preliminary trials (data not shown) using stimuli from several candidate vectors. The goal was to ensure sigmoidal detection curves, which requires that the lowest contrast stimuli are not reliably detected. From the time of stimulus presentation, monkeys had 290 ms to make a saccade to the location of the target to indicate correct detection of the stimulus. This time window allows sufficient time to saccade to our low contrast stimuli while still encouraging the animals to make rapid decisions. Correct detections resulted in delivery of five drops of liquid reward. This large reward was implemented to encourage the animals to indicate a

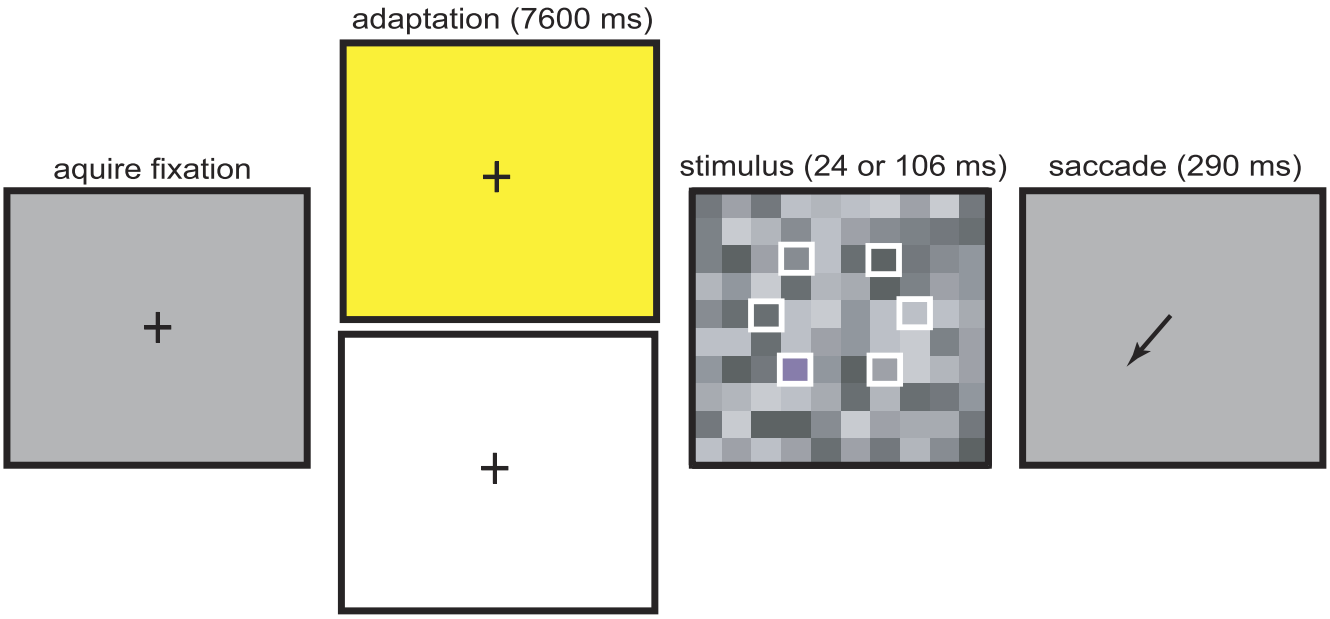

Figure 2. Tritan line calibration task. At the start of each trial, monkeys fixated a central cross on an EEG background. During fixation, a yellow or white bright adapting background was turned on. At the end of the fixation period the fixation cross was turned off and simultaneously a target was presented embedded in a screen of $1^\circ \times 1^\circ$ gray squares. The target square appeared randomly in one of six possible locations on each trial (unfilled white squares, not visible to monkeys). Target color was randomly selected on each trial from one of the eight possible test steps. To indicate detection, animals had to initiate a saccade to the location of the target.

correct detection. This was done at the expense of further limiting the number of trials animals will perform before satiation but was necessary to maintain motivation throughout the long and difficult tritanopia trials.

In this paradigm, animals generally attempted nearly every trial, ensuring a reasonable maintenance of adaptation throughout data collection. Near the end of a session, if the monkey stopped reliably performing trials or did not attempt trials for a few minutes, data collection was stopped for the day.

Measuring detection thresholds

The task was designed to find detection thresholds along chosen candidate tritan vectors. Detection thresholds were found in a staircase manner using stimuli from the test step points (Figure 3B). The idea was to find the test step, or distance from EEG in MB space, for stimuli on a candidate tritan vector to be reliably detected. During transient tritanopia, the candidate vector with the highest detection threshold is the true tritan line at the tested spatial location. Candidate vectors range from 0° to 24°, spaced 2° apart. We focused on testing candidate vectors from 8° to 24° because previous studies using the transient tritanopia method for finding a tritan line have found the true tritan line to lie near this range (Smithson et al., 2003; A. J. Anderson & Carpenter, 2008).

Test steps for finding detection thresholds are indicated by the equally spaced curves spanning candidate vectors (Figure 3B). Moving along a candidate tritan vector away from EEG represents steps of increasing S-cone chromatic contrast. Test steps at greater distances from EEG should become easier to detect as their chromatic contrast from the background increases.

Percent correct was calculated as the ratio of correct stimulus detection trials to attempted trials. A trial was considered attempted if the monkey maintained fixation up to stimulus presentation. Trials aborted before stimulus presentation were not included in the analysis. Trials were considered correct if monkeys made an eye movement to the stimulus location within the allotted 290 ms after stimulus onset. Saccades had to land within approximately a $2^\circ \times 2^\circ$ window centered on the stimulus location to be considered correct. If monkeys made a saccade to any other location or did not initiate a response within 290 ms, the attempted trial was considered an error trial. We included "no response" trials in the analysis as error trials because it is unlikely the animals would fail to indicate a detected target. The reward paradigm offers a large reward for correct detection. It is doubtful that the monkeys would perform a long fixation of a bright background for little reward only to choose not to take the large reward offered for correct detection.

Detection thresholds were computed from plots of percent correct target detections versus stimulus

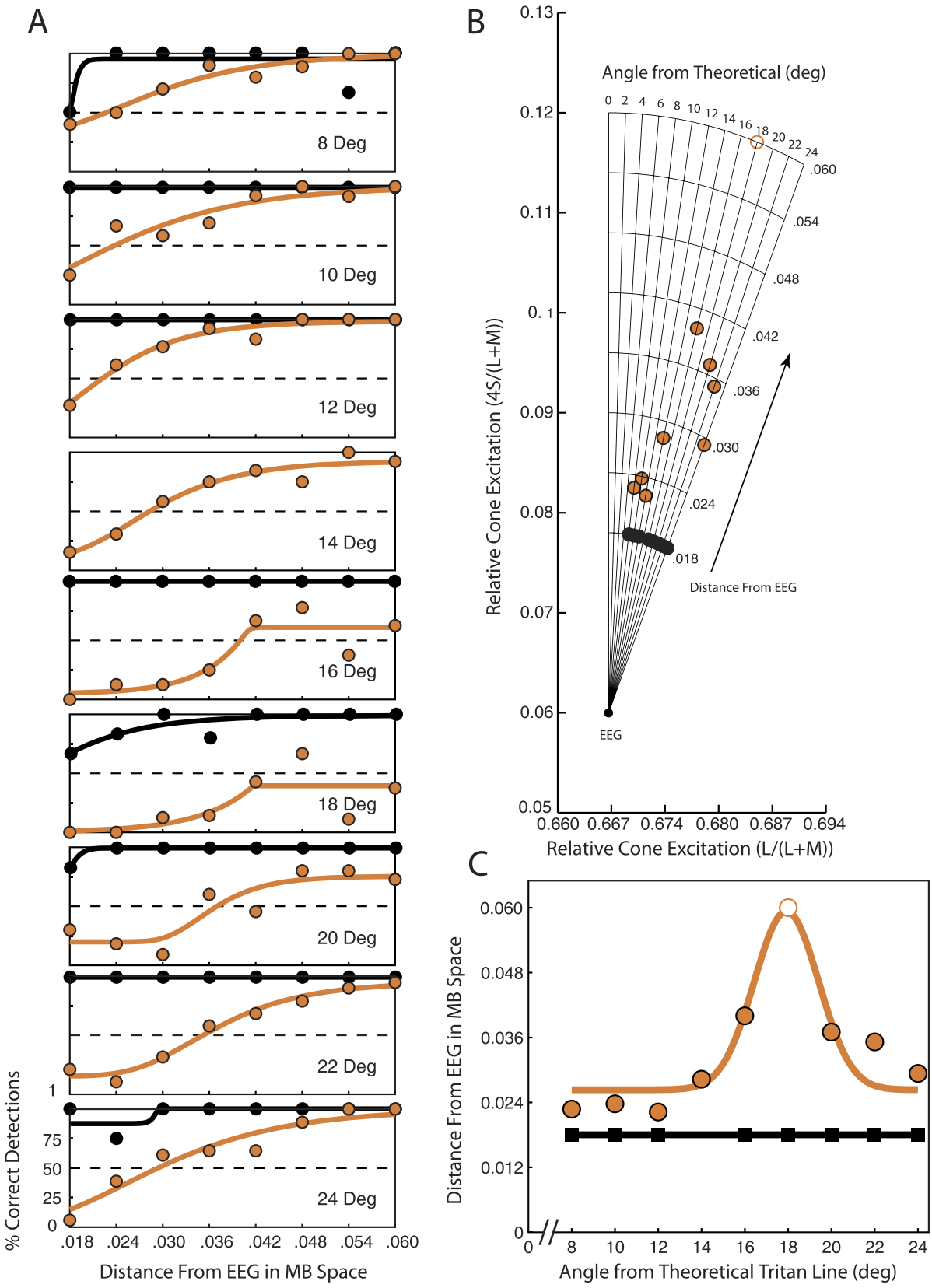

Figure 3. Tritan line calculation from detection thresholds at one spatial location (down left) for monkey FS. Orange circles show data collected after adaptation to the yellow adapting background. Black circles show data collected after adaptation to the white adapting background. (A) Percent correct detections plotted versus distance of the test step stimulus color from EEG in MB space for nine

→

distance from EEG in MB space for each candidate tritan vector (Figure 3A). Moving along the x-axis represents increasing distance from EEG, i.e., increasing chromatic contrast between the target stimulus and gray background squares. The monkeys' detection percentage generally increased as contrast increased. Behavioral performance in a detection task such as this can be expected to follow a sigmoidal function. We therefore fit a least-squares six-parameter generalized logistic function to the data points as follows.

$$A + \frac{(K - A)}{\{1 + Q*\exp[-B(x - M)]\}^{(1/V)}} \quad (1)$$

The parameters A and K represent the lower and upper asymptotes, respectively. These were constrained to lie between zero and one. The parameter M represents the shift of the curve from zero and was constrained to lie between 0.018 and 0.060. The other parameters modify the shape and steepness of the fitted curve and were constrained to be zero or positive. To compute thresholds, we found the point at which the fitted curve reached 50% correct detections (dashed horizontal lines in Figure 3A). The corresponding distance from EEG required for the fitted curve to reach 50% was considered to be the detection threshold for the candidate tritan vector tested (Figures 3A, B). If the fitted curve never reached 50% correct (as in the 18° panel of Figure 3A) a threshold of 0.060 was assigned. Thresholds assigned a value of 0.060 are indicated by open circles (Figures 3B-C, 4, and 5).

Thresholds were determined separately for tritanopia trials (Figure 3, orange points and curves) and control trials after adaptation to the white background (Figure 3, black points and curves). Threshold values were then plotted as a function of candidate tritan vector angle from zero (Figure 3C). This function is expected to produce a single peak of greatest detection threshold for tritanopia trials. Tritanopia data points were fitted with a least-squares four-parameter Gaussian function as follows.

$$A*\exp\left(-\frac{x - B}{C}\right)^2 + D \quad (2)$$

The parameter A affects the magnitude of the curve and was constrained to lie between 0.01 and 0.06. Parameter D indicates the minimum value of the fit and was constrained between zero and 0.048. Combined, the constraints on A and D kept the values of the fitted curves within the range of thresholds observed and tested. Parameter C controls the width of the Gaussian function and was constrained between 1.5 and 6.5. This window allowed the curves to rise in correspondence with sharp increases in detection threshold. The parameter B indicates centering of the curve, which is the peak of the fitted function. B was constrained to lie between eight and 24 in correspondence with our tested range of candidate tritan vectors. The value of B was used to define the peak of the function and thus the tritan vector with greatest threshold.

We characterized goodness of fit for the Gaussian functions by computing the ratio of the root mean square error (RMSE) of the fitted Gaussian and the RMSE of the mean. Values of this RMSE ratio equal to one indicate that the mean fits the data as well as the fitted Gaussian. Values less than one indicate the Gaussian fit is better than the mean whereas values greater than one indicate that the Gaussian fit is worse than the mean. RMSE was computed using degrees of freedom equaling the number of data points tested (nine for monkey FS and seven for monkey CA) minus the number of model parameters (four for fitted Gaussians and one for the mean).

Control trials were expected to produce flat detection thresholds even below our threshold of 0.018 as found by Smithson et al. (2003) in human subjects. Therefore these trials were fitted with a least-squares linear function. Trials collected for a single candidate tritan vector were combined across sessions for which the same vector was tested. This analysis was performed separately for each candidate tritan vector at each of the six spatial locations using each of the two adaptation backgrounds for each monkey.

Results

Detection thresholds indicate the observer's true tritan line

We used a transient tritanopia based paradigm to define S-cone isolating stimuli. In this paradigm,

←

candidate tritan vectors. Orange and black curves are the least-squares logistic fits to the data. Dashed horizontal lines at 50 indicate chosen detection percentage threshold. (B) Detection thresholds computed from the detection curves in A and plotted in scaled MB space. Each point on a candidate tritan vector indicates the detection threshold for that vector as determined from the data in A. (C) Detection thresholds from B are plotted as a function of the candidate tritan vectors (i.e., angle from theoretical tritan line). Here the vertical axis indicates threshold distance from EEG shown in B while the horizontal axis indicates the candidate vector tested. Data points for tritanopia trials were fitted with a least-squares Gaussian function (orange curve) to determine the peak. Data points for control trials were fitted with a least-squares linear function (black line).

adaptation to a yellow background produces temporary insensitivity to S-cone activation. We measured detection of near S-cone isolating stimuli chosen from candidate tritan vectors during transient tritanopia. The tritan vector is a line in color space along which only S-cone excitation is modulated. We found detection thresholds for each candidate tritan vector at six spatial locations in two monkeys. To measure detection thresholds, we presented stimuli chosen from along each candidate tritan vector. Stimuli were varied in chromatic contrast in a staircase fashion. Stimulus contrast increases with distance from equal energy gray (EEG) in Macleod-Boynton (MB) space. Stimuli further out are easier to detect than those near the EEG point. The goal of testing these points is to find the minimum distance from EEG required to produce reliable detection along each candidate vector. Greater distance from EEG indicates a higher detection threshold and greater transient tritanopia effect. The true tritan line is the candidate tritan vector with the highest detection threshold during conditions of transient tritanopia (i.e., after adaptation to the yellow background). An S-cone isolating stimulus is one chosen from this true tritan line.

Data were collected and analyzed separately for control trials after adaptation to a white background (Figure 3, black points and curves) and tritanopia trials after adaptation to a bright yellow background (Figure 3, orange points and curves). Results are shown for nine candidate vectors at a single spatial location for monkey FS (Figure 3). The candidate vector on which the orange threshold point is furthest from EEG (the 18° vector in Figure 3B) is the one nearest the true tritan line. When threshold distances are plotted in MB space (Figure 3B) it is clear that contrast must increase the most along the 18° candidate vector to produce stimulus detection. Because transient tritanopia affects sensitivity maximally for true S-cone stimuli, this means the 18° vector is most closely aligned with the animal's true tritan line for this spatial location. Control trials show no detection thresholds above 0.018 across candidate vectors.

The data shown in Figure 3B are summarized in Figure 3C. Plotting thresholds as shown in Figure 3C makes it easier to see the peak threshold value. In this example a 17.9° tritan vector has the highest detection threshold as given by the peak of the Gaussian fit. Therefore a 17.9° tritan vector is the true tritan line for monkey FS at this location in space.

Determining spatially specific tritan lines

True tritan lines were determined for six spatial locations. Detection thresholds were calculated iteratively for each candidate tritan vector, spatial location, and monkey (Figures 4 and 5). This nested procedure of computing detection thresholds was performed separately for control trials and tritanopia trials. In each daily session a single candidate vector was tested across all six locations on either control or tritanopia trials. Each point represents performance measured across all sessions in which a particular candidate vector was tested. Large panels show data collected at the six spatial locations indicated by the central illustration.

Both animals displayed steady stimulus detection (black squares) during control trials as indicated by a flat fit with a linear least-squares function (black lines). For all locations except Figure 5, lower left, and Figure 4, upper left, detection during control trials exceeded 50% even at the lowest stimulus contrast tested. This constrained these trials to flat lines at 0.018 units from EEG and placed an upper bound on detection threshold in the absence of transient tritanopia. Separate analyses demonstrate that thresholds did not systematically vary across candidate tritan vectors during control trials (see online supplementary materials) as shown in human subjects (Smithson et al., 2003). In contrast, detection threshold was markedly increased above 0.018 during transient tritanopia (orange circles) and thresholds systematically varied across test vectors with a peak for a specific candidate vector value as indicated by the least-squares Gaussian fits (orange curves). Increased threshold after adaptation to the yellow compared to white control background demonstrates that transient tritanopia is taking place. This is true across spatial locations and candidate vectors for both monkeys. Peaks of detection threshold on orange curves indicate the true tritan line at that spatial location.

A few stimulus locations did not produce clear results. Monkey FS rarely detected the target, regardless of contrast, during transient tritanopia for the up-right location (Figure 4, top right panel). There was no clear relation between contrast and detection so there are no meaningful thresholds for candidate vectors. Thresholds appear similarly and extraordinarily elevated across all candidate vectors. The fitted curve at the down-right location is also relatively flat without an evident peak (Figure 4, bottom-right panel). For monkey CA, the down-left location (Figure 5 bottom left panel) and the up-right location (Figure 5 top-right panel) both contain considerable variation from point to point. For the up-right location, this is largely due to the low threshold outlier point for the 20° candidate vector. Data point variation from the fitted curve is especially problematic for the down-left location where the control data are also more variable than at the other locations. This indicates that monkey CA did not perform accurately during trials at this location even during the easier control trials. These unreliable control

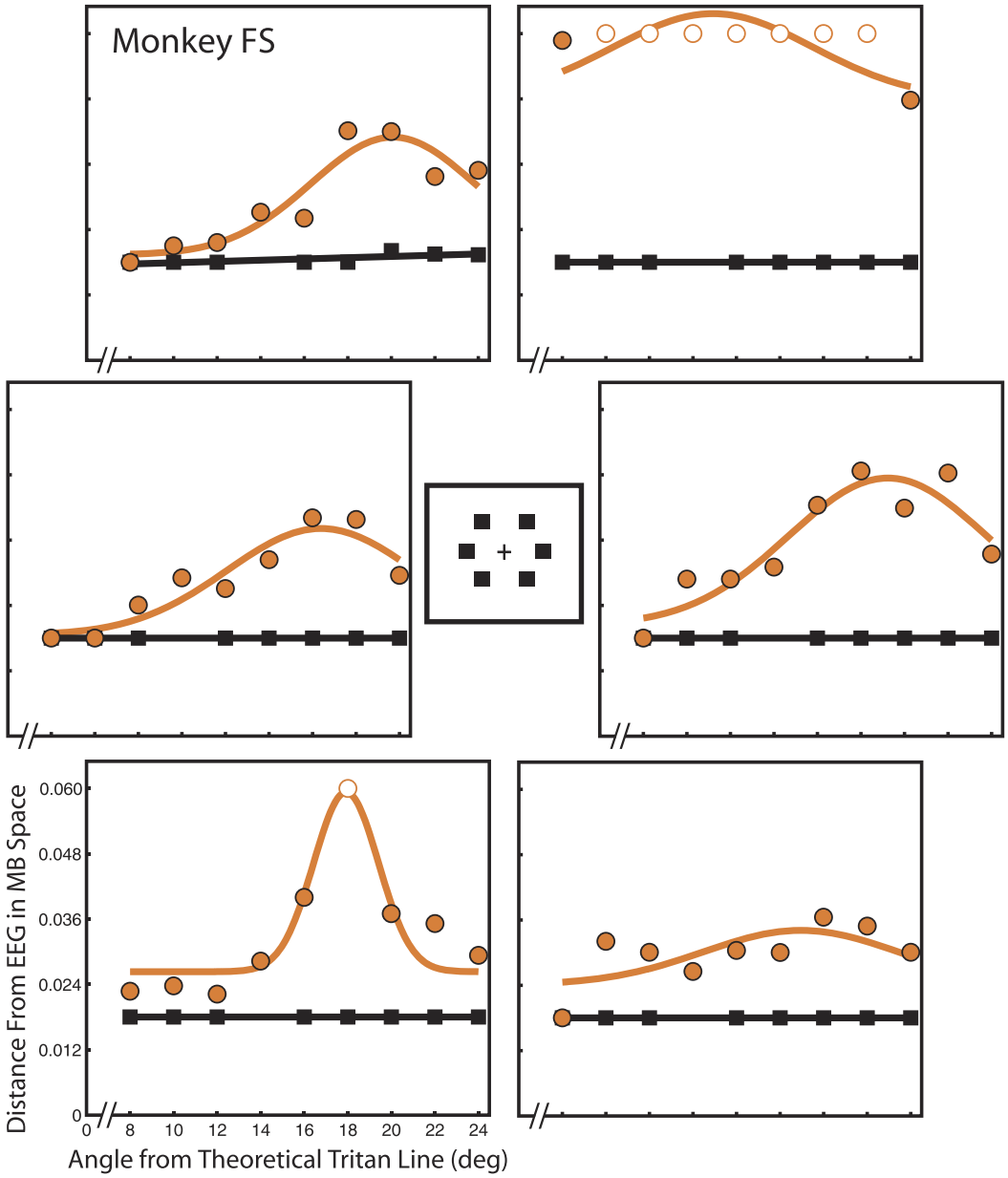

Figure 4. Detection thresholds for monkey FS. Each panel shows detection thresholds for monkey FS at one of the six spatial locations tested. All locations were 4° eccentricity. Vertical axes represent detection threshold as distance from EEG in scaled MB space. Horizontal axes indicate candidate tritan vector angle. Orange circles indicate data collected during tritanopia trials. Orange curves show least-squares Gaussian fits. Gaussian peaks indicate the angle of greatest threshold increase and thus reveal true S-cone isolating stimuli. Black squares indicate data collected during control trials. Black lines show least-squares linear fits.

trials suggest that transient tritanopia trials at this location may also be unreliable. In these instances, the RMSE ratio is near or above one at these locations, indicating a poor fit (Table 1). The RMSE ratio at the down-right location for monkey CA is equal to one, indicating that the Gaussian fit is no better than a flat line at the mean. This flatness is due to the relatively low threshold elevation at this location.

The remaining locations (7/12) in both monkeys produced good Gaussian fits that reveal threshold peaks indicative of the true tritan line with corresponding low threshold control trials. A summary of true tritan lines for each monkey at each location in space is shown in Table 1. These angles are given as the peaks of the fitted Gaussian function (Parameter B in Equation 2).

Behavioral analysis

We wanted to know whether the variability in detection threshold distance across locations could be

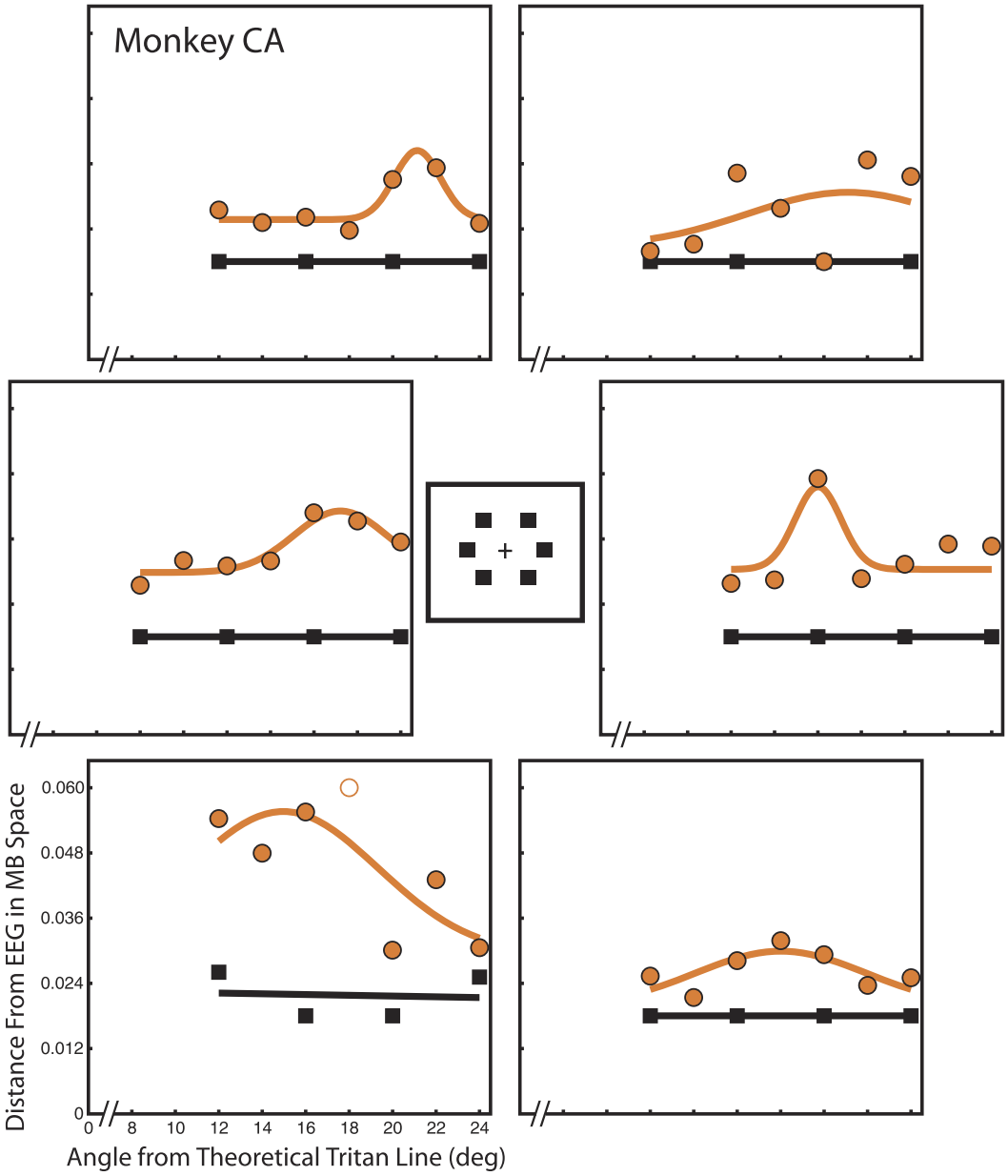

Figure 5. Detection thresholds for monkey CA. Same format as Figure 4. All locations were 6° eccentricity.

related to bias on the part of the monkeys. We analyzed saccade endpoints to determine whether bias was present in the animals' behavior. Bias should appear as a preference to choose certain target locations more or less often than others on error saccade trials. During these trials, the monkeys typically appear to guess a potential target location. Bias toward a particular location might result in decreased detection thresholds at that location as the animal is more likely to correctly "guess" that target location even though he did not detect the target. Conversely, bias away from a particular location might result in increased detection thresholds.

We plotted saccade endpoints for correct and error trials in order to examine the monkeys' performance and location bias (Figure 6). To quantify performance and bias we used chi-squared tests of homogeneity. Within a given trial type (individual panels in Figure 6) the endpoint distribution was compared to the expected (unbiased) proportion of 1/6 at each location. Distributions were also compared between trial types. These comparisons were followed by post-hoc multiple comparisons between corresponding locations using the Goodman procedure (Goodman, 1964; Franke, Ho, & Christie, 2012) with p-value = 0.05.

We set the unbiased proportion at 1/6 for attempted saccade trials because monkeys typically made saccades

Location	Monkey FS	Monkey CA
Up right	14.9* (1.3057)	21.1 (1.2857)
Straight right	19.2 (0.4765)	16.0 (0.7941)
Down right	19.0 (0.9060)	18.0 (1.0000)
Down left	17.9 (0.4040)	15.0 (0.9333)
Straight left	20.4 (0.4462)	21.2 (0.5000)
Up left	20.1 (0.4550)	21.1 (0.4091)

Table 1. Calibrated tritan vectors by monkey and location. Summary of calibrated tritan axes as determined from Gaussian fit function peaks for both monkeys at all spatial locations. Tritan axes are given in clockwise degrees angular rotation from the theoretical tritan vector. Numbers in parentheses indicate goodness of fit for each Gaussian calculated as the ratio between RMSE fit and RMSE mean. Smaller numbers indicate better fit. Values near one indicate especially poor fits.
* - Indicates that the peak at this location was largely arbitrary and not fitted to reliable data.

to locations at or near potential target locations even when they did not detect the target (Figure 6C and G). This is especially true in monkey CA, who had very few no response error trials (Figure 6G, H black triangles). In contrast, monkey FS exhibits a large number of no response tritanopia trials (Figure 6C, black triangles). As one might expect, the largest number of these (360) occurred after target presentations at the up-right location which he was strongly biased against. It is reasonable to assume that his unbiased performance would lie near the expected value of 1/6.

We found that correct performance of monkey FS during tritanopia trials (Figure 6A) was not equal for all locations ($p < 0.0001$). Monkey FS rarely performed correctly on up-right trials and exceeded expectation on up-left trials. This correct performance distribution is similar to his location bias as evidenced by error trials (Figure 6C) in which he showed bias ($p < 0.0001$) away from the up-right location and toward the up left. In an effort to discover whether error saccade bias is predictive of correct performance, we directly compared correct trials to error trials. We found that the difference between correct and error trial bias lies only in bias being less extreme at the upper locations during correct compared to error trials (both locations, $p < 0.05$). This is largely because

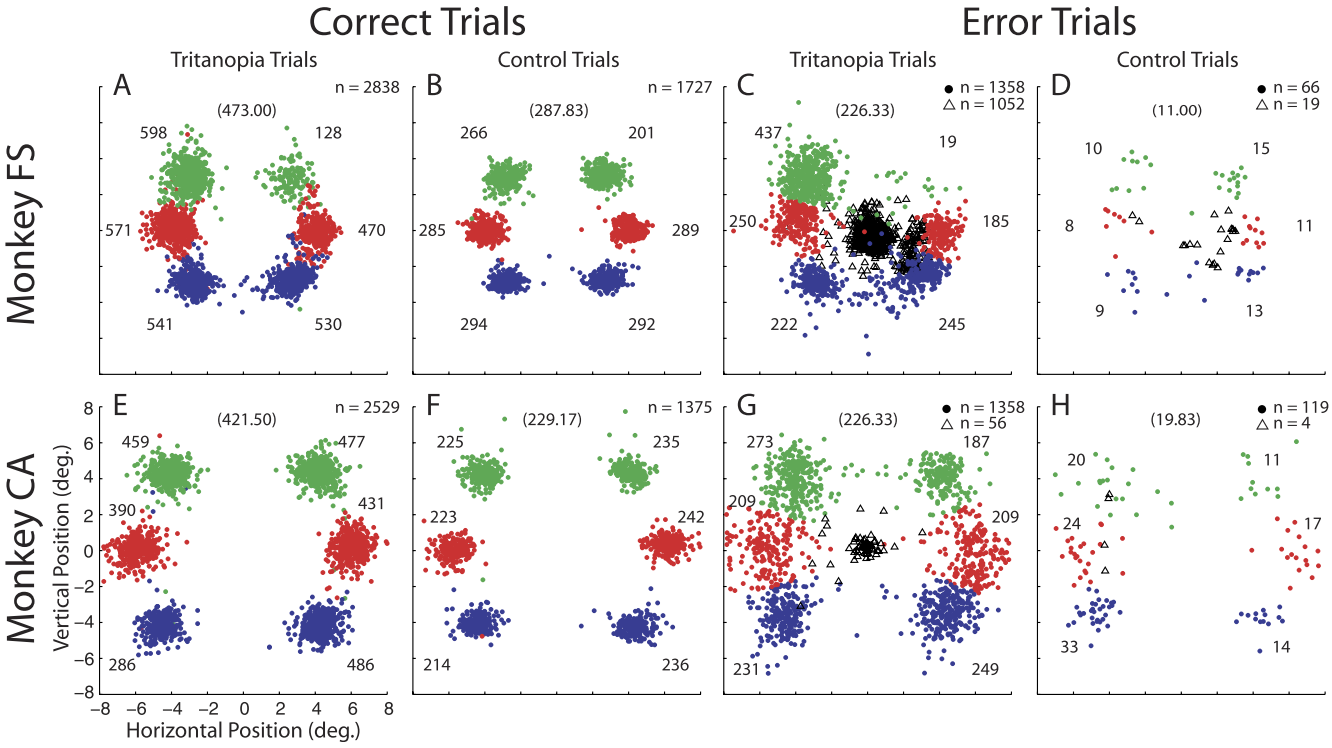

Figure 6. Saccade endpoints during tritanopia and control trials. Endpoints are shown for all candidate tritan vectors and stimulus contrasts. Colored circles indicate trials in which a saccade was attempted. Color code for correct trials shows endpoints corresponding to target presentations at each of six locations. Endpoints far away from their colored cluster are due to occasional eye position drift but represent correct decisions and are placed in the analysis with their corresponding cluster. The average position of correct saccade endpoints for each location was used to classify error endpoints. Error saccade endpoints were classified as being directed to one of the six possible target locations based on the nearest endpoint during correct trials. Numbers near each cluster give the number of endpoints. Numbers in parentheses at the top of each panel give the expected (unbiased) number of endpoints for each location. The unfilled black triangles show eye position 300 ms after target presentation for error trials in which no saccade was attempted.

monkey FS almost never chose the up-right target unless he was correct. The distributions both trend in the same direction, suggesting that bias played a role in his performance.

Monkey CA also showed unequal performance across locations ($p < 0.0001$) during correct transient tritanopia trials (Figure 6E). This difference is largely due to a low number of correct detections at the down-left location. Monkey CA further showed bias during error trials (Figure 6G, $p < 0.001$). Interestingly, bias during error trials was strongest away from the up-right location and toward the up-left location. This bias does not predict the performance seen during correct trials. Error trial bias significantly differed from correct trial performance at the up-right and down-left locations (both locations, $p < 0.05$). At these locations where performance and bias are at odds, it appears monkey CA was simply not good (down left) or very good (up right) at detecting the target. His performance at the remaining locations did not differ from his error trial bias. This can be seen in slightly better performance at the up-left and down-right locations (Figure 6E) corresponding to his small bias to these locations (Figure 6G).

Bias was much less evident during the easier control trials. Monkey FS still exhibits nonuniform correct performance (Figure 6B, $p < 0.001$) which is again strongest away from the up-right location. Enhanced performance at the up-left location is no longer evident. Monkey CA showed no variability in location performance (Figure 6F, $p = 0.8039$). During control error trials (Figure 6D) no bias was observed for monkey FS ($p = 0.6860$). This distribution differed significantly from his biased selections during tritanopia error trials ($p < 0.0001$) as he increased selection to the up-right target and decreased it to the up-left one (both ps $<$ 0.05). Error control trial bias was present for monkey CA (Figure 6H, $p = 0.0078$) and this bias differed from that during tritanopia error trials ($p = 0.0181$). The bias change between tritanopia and control trials was not significant for any individual location comparison and does not materialize in his unbiased correct performance.

Any bias observed in these data is inherent to the animals' behavioral patterns and preferences. With the exception of the down-left location for monkey CA, both animals performed very accurately for all locations during control conditions (Figures 4 and 5, black squares) after adaptation to the white background. They also demonstrate far less bias during these control trials. Therefore, the origin of any bias cannot be explained by scotoma or major visual deficit at these areas.

Endpoint biases revealed in this analysis do not reliably predict calibration quality at a given location. The only major exception is the very strong bias of monkey FS away from the up-right location, which resulted in so few detections that the calibration could not really be performed there. His bias to the up-left target may explain the slightly lower threshold peaks at this location, though the effect appears small (Figure 4). His bias does not account for his decreased detection thresholds to the down-right location, to which he showed no bias. Monkey CA's (Figure 5) tritanopia error bias toward the up-left target may have also slightly decreased the threshold peak for the up-left location. However, his elevated thresholds for the down-left target would not be predicted from his tritanopia error trials which show no bias away from this location. Monkey CA also shows rather flat thresholds for the up-right target which would not be predicted based on his bias away from this location. These results suggest the monkeys were simply unusually good or bad at detecting targets in some locations.

Both monkeys show variability in performance and error saccade bias across spatial locations. Behavioral biases are only able to explain calibration performance in extreme cases. There is a trend for biased locations to show decreased or elevated detection thresholds at some locations. However, deviations in performance across locations cannot be reliably predicted based on bias observed during error trials. For bias to affect our estimated tritan vectors independent of location would require the monkeys to be biased in a test vector direction dependent manner. This seems unlikely as the rapid stimulus presentation gives the monkeys little time to react and individual vectors were tested across days. This suggests that bias plays little or no role in our calibration results at most locations tested.

Discussion

We have shown that S-cone isolating stimuli can be defined in monkeys by taking advantage of transient tritanopia. Transient tritanopia occurs after adaptation to a bright yellow background. It produces selective desensitization to S-cone input which can be used to determine an observer's true tritan line. Our method is modeled after the technique introduced by Smithson et al. (2003) to identify tritan lines in human subjects. This method for finding a tritan line and determining truly S-cone isolating stimuli has never before been performed on nonhuman subjects. The ability to stimulate S-cones selectively in awake behaving monkeys is important for two reasons. This approach will allow future behavioral studies on responses to S-cone stimuli in monkeys to have direct relevance to previous psychophysical work in humans. Further, defining S-cone isolating stimuli in monkeys allows physiological studies not possible in humans.

Methodological differences from calibrations in humans

The transient tritanopia calibration procedure described here differs in three main ways from those previously used on human subjects (Sumner et al., 2002; Smithson et al., 2003; Smithson & Mollon, 2004; Sumner et al., 2004; Sumner et al., 2006; A. J. Anderson & Carpenter, 2008; E. J. Anderson, Husain, & Sumner, 2008; Bompas, Sterling, Rafal, & Sumner, 2008; Bompas & Sumner, 2008). First, our procedure requires that subjects indicate detection by performing a saccade to a single briefly presented target embedded in luminance noise. In contrast, many human studies have used verbal report to indicate detection of Ishihara rings of stimuli. To determine thresholds, we fit psychometric curves indicating percent correct stimulus detection. These curves were used to determine the point at which the stimulus was reliably detected by the animals.

A second difference from the procedures used in humans is that we did not use an initial adaptation period to induce transient tritanopia. We began each experimental session by running approximately 10 trials using the standard 7.6 second adaption to a yellow background at the beginning of each trial. After these initial trials, data collection begun using the same trial parameters. To maintain adaptation, data were collected only so long as animals were reliably performing trials. Previous calibrations in humans assume that subjects will continue to perform trials so long as it is asked of them with little error or few unattempted trials. These human studies used an initial adaptation period of 1–2 minutes to induce transient tritanopia. After initial adaption, trials were run with about 7.6 seconds of adaptation per trial to maintain transient tritanopia. We found that the initial adaption prolongs the already more difficult task of calibrating a tritan line in monkeys. Adaptation would need to be repeated if the monkey did not perform the task for several trials. Our method produced sufficient adaptation for transient tritanopia without initial adaption. In both animals, detection thresholds were clearly elevated after adaption to the yellow compared to white background.

A third difference was the method used for luminance calibration. We photometrically calibrated our S-cone stimuli for equiluminance with the background. Several previous studies have instead used psychophysical luminance calibration, such as the minimum motion procedure for determining equiluminance (Anstis & Cavanagh, 1983). We did not psychophysically calibrate equiluminance for three reasons. (A) Our preliminary results with the minimum motion technique in one monkey (data not shown) were inconsistent at the eccentric locations of our stimuli as has been reported previously in monkeys (Logothetis & Charles, 1990). Additionally, this psychophysically estimated equiluminant point ultimately differed little from measured photopic equiluminance. (B) Psychophysical luminance calibration results can depend on spatial and temporal properties of the stimulus (Anstis & Cavanagh, 1983; Cavanagh, MacLeod, & Anstis, 1987; Logothetis & Charles, 1990) and vary with eccentricity (Bilodeau & Faubert, 1997). (C) The equiluminant point differs from one neuron to the next (Schiller & Colby, 1983). This implies that in any future physiological experiments using the S-cone calibration technique presented here, stimulus luminance would need to be calibrated before recording each individual neuron. We reasoned that any small measurement inaccuracy would be masked by using luminance noise that varied over a relatively wide range of values (± 2 cd/m^2) from the target luminance. We found that omitting psychophysical luminance calibration simplifies the procedure while still producing results dependent on chromatic contrast.

Comparison to calibrations in humans

Our calibration results in two monkeys are similar to tritan line calibrations in humans (Smithson et al., 2003; A. J. Anderson & Carpenter, 2008). These previous studies found that actual tritan lines are typically shifted toward red (clockwise rotation of the vector from theoretical), as expected (Sumner et al., 2004). Across four subjects, Anderson and Carpenter (2008) identify tritan lines of 10.6°, 11.8°, 14.5°, and 17.7° clockwise rotation from the theoretical line. With two subjects, Smithson et al. (2003) found tritan lines of 7.8° and 9.5° clockwise rotation when using an adaption background similar to ours. Tritan lines in monkeys were actually rotated slightly further, but critically, they trend in the same direction. They ranged from 15.0° to 21.2° rotation in monkey CA and 17.9° to 20.4° rotation in monkey FS (Table 1), excluding the unattempted location (Figure 4, upper right).

The difference in calibrated tritan lines between humans and monkeys might be attributable to eccentricity and corresponding macular pigment density. The two studies above both used annular stimuli that spanned an entire visual quadrant. Furthermore, the stimulus annulus covered an area from 3° to 5° eccentricity. Here we tested stimuli that were single points centered at either 4° or 6° eccentricity. Macular pigments in humans and monkeys have similar absorption spectra and a higher density near the fovea. However, it appears that human macular pigment may extend further from the fovea than in monkeys (Snodderly et al., 1984a; Snodderly et al., 1984b; Trieschmann et al., 2007). A lower density of macular

pigment in the periphery and/or more eccentric test locations would result in the observed greater shift toward red in the calibrated tritan line seen in our animals.

Differences between locations and animals

Calibrated tritan lines in both monkeys were qualitatively very similar. They ranged from 15.0° to 21.2° rotation in monkey CA and 17.9° to 20.4° rotation in monkey FS (Table 1), excluding the unattempted location (Figure 4, up right). Individual variations at successfully calibrated locations are to be expected. S-cone isolating stimuli vary between observers due to variations in macular pigment, lens optical density, cone sensitivity, and chromatic aberration (Sumner et al., 2004). Both monkeys showed evidence of bias toward or away from one to two locations, particularly during the more difficult transient tritanopia trials. Although bias can explain variability in calibration quality at some locations, it cannot account for all of them, particularly the flatter curves for monkey CA up right and monkey FS down right. At these locations where bias does not play a major role, it appears the monkeys were simply too effective at target detection to produce good calibrations. Nonetheless, a peak is evident and this could possibly be accentuated by altering specific trial parameters that would increase detection threshold. For example, increasing the strength of transient tritanopia by brightening the adaption background would likely make targets more difficult to detect. Alternatively, decreasing target presentation time has a similar effect. Unfortunately, changes like these would in turn make target detection at other locations more difficult as well. We wanted to keep trial parameters identical for each test location so that target location was unpredictable. The parameters chosen here sought a balance that would produce good results at as many locations as feasible.

S-cone contributions to visual subsystems

Signals from the three cone types are carried from retina to the brain by different classes of ganglion cells that largely maintain segregation through the thalamus and into cortex. This segregation leads to a number of visual subsystems. One intriguing instance of such segregation is the pathway for luminance perception (Lee, 2011). Luminance perception arises from addition of signals from L- and M-cones, but not S-cones (Eisner & MacLeod, 1980). Luminance perception in primates has been linked to the magnocellular layers of the lateral geniculate nucleus (LGN) (Lee, Martin, & Valberg, 1988; Lee, 2011). Neurons in the magnocellular layers of the LGN sum inputs from L- and M-cones but rarely or not at all from S-cones (Schiller & Malpeli, 1978; Derrington, Krauskopf, & Lennie, 1984; Sun, Smithson, Zaidi, & Lee, 2006; Field et al., 2010). S-cone signals are carried by their own class of retinal ganglion cell which projects almost exclusively to the koniocellular LGN layers (Dacey & Lee, 1994; Hendry & Reid, 2000; Klug, Herr, Ngo, Sterling, & Schein, 2003; Dacey, 2004; Dacey et al., 2005; Tailby, Solomon, & Lennie, 2008). However, it is possible that S-cone input to the magnocellular LGN is simply weaker than that of L- and M-cones (Derrington et al., 1984; Ripamonti, Woo, Crowther, & Stockman, 2009). With calibrated S-cone isolating stimuli, L- and M-cone input can be held constant using an isoluminant gray background while changes in the S-cone opponent direction are manipulated by presenting a calibrated S-cone stimulus. The ability to define S-cone stimuli in monkeys affords the opportunity to test aspects of segregated S-cone processing physiologically in a novel way.

Physiological extensions of psychophysical studies

An important set of questions center around the idea that the superior colliculus (SC) does not receive input from S-cones (de Monasterio, 1978; Schiller et al., 1979; Sumner et al., 2002). The SC is thought to play a central role in visually guided behavior, such as orienting in space and the control of eye movements. The lack of S-cone input to the SC was recognized by Sumner et al. (2002) as an opportunity to test collicular function. The authors reasoned that the SC could be effectively "lesioned" during behavioral studies in humans by using visual stimuli that it cannot perceive. Such collicular lesions are performed by presenting calibrated S-cone isolating stimuli.

The use of S-cone stimuli to block visual input to the SC has been directed toward a number of phenomena, including involuntary attention, the oculomotor distracter effect, and inhibition of return (Sumner et al., 2002; Sumner et al., 2004). In these human psychophysical tests, reaction times in trials using S-cone isolating stimuli are compared with trials using L-cone, M-cone, or luminance stimuli. This technique has been applied to show that these phenomena are affected when S-cone stimuli are used. The conclusion is that the SC plays a role in involuntary attention, the oculomotor distracter effect, and inhibition of return.

Neural mechanisms underlying the effect of using S-cone stimuli on involuntary attention, the oculomotor distracter effect, and inhibition of return could be studied with the availability of monkey specific tritan

line calibrations. One could perform the experiments done previously in humans using calibrated S-cone isolating stimuli while monitoring neuronal activity in monkeys. If the SC underlies these phenomena, activity there should reflect the differences in behavior observed when S-cone stimuli are used compared to luminance stimuli.

Physiological extensions of clinical studies

Clinical studies have also relied on the S-cone stimulus strategy introduced by Sumner et al. (2002). S-cone stimuli have been used to assess SC-mediated interhemispheric transfer in split-brain patients by measuring reaction time for stimuli detected by one hemisphere (Savazzi & Marzi, 2004; Savazzi et al., 2007). They concluded that the SC is important for these patients to maintain interhemispheric transfer of sensorimotor information. A second clinical application of the S-cone approach is in the study of blindsight, where it has been suggested that the SC plays a role in residual vision of patients with visual cortical lesions (Leh et al., 2006; Leh et al., 2010). The role of the SC in interhemispheric transfer and blindsight could be investigated by recording neural activity in the SC of monkeys using calibrated S-cone isolating stimuli. For interhemispheric transfer, one could measure whether S-cone stimulus responses can appear in both sides of the SC. To test SC-mediated blindsight, lesions to primary visual cortex could be made. Activity in SC could be recorded and compared between calibrated S-cone isolating and luminance stimuli to provide a more concrete basis for these important clinical studies.

Conclusions

The perceptual reports of nonhuman primates can be used to perform psychophysical calibrations of S-cone isolating stimuli. S-cone isolating stimuli can be calibrated separately at several spatial locations for individual monkeys. These S-cone isolating stimuli were determined by finding a stimulus whose detection threshold was maximally elevated during transient tritanopia. This calibration is specific to both location and animal. S-cone stimuli were successfully determined at most locations tested in each monkey. This technique in monkeys will allow physiological tests of S-cone function not previously possible. It provides a direct link to calibrations in previous human studies which should allow it to elucidate the neural foundations of phenomena such as blindsight that have attracted great interest yet remain unresolved.

Keywords: tritan line, blue cone, behavioral calibration, monkey, transient tritanopia

Acknowledgments

We thank K. McCracken and Dr. Kevin Hitchens for technical assistance and our colleagues at the Center for the Neural Basis of Cognition for discussion and comments. We also thank Dr. R. Desimone for provision of the CORTEX program developed in his laboratory at NIMH. This work was supported by National Institutes of Health Grants EY-12032 and MH-45156. Technical support was provided by core grant EY-08908, and collection of MR images was supported by P41RR-03631. N. Hall was also supported by a National Science Foundation IGERT award (DGE 0549352).

Commercial relationships: none.
Corresponding author: Nathan Hall.
Email: njh5@cnbc.cmu.edu.
Address: Department of Neuroscience and Center for the Neural Basis of Cognition, University of Pittsburgh, Pittsburgh, PA, USA.

References

Anderson, A. J., & Carpenter, R. H. S. (2008). The effect of stimuli that isolate S-cones on early saccades and the gap effect. *Proceedings of the Royal Society London B Biological Sciences, 275,* 335–344.

Anderson, E. J., Husain, M., & Sumner, P. (2008). Human intraparietal sulcus (IPS) and competition between exogenous and endogenous saccade plans. *NeuroImage, 40*(2), 838–851, http://www.sciencedirect.com/science/article/B6WNP-4R40SM9-6/2/8ab29461e24dd35ec0690e2a94fdab32.

Anstis, S. M., & Cavanagh, P. (1983). A minimum motion technique for judging equiluminance. In J. D. Mollon & L. T. Sharpe (Eds.), *Colour vision: Physiology and psychophysics* (pp. 156–166). London: Academic Press London.

Bilodeau, L., & Faubert, J. (1997). Isoluminance and chromatic motion perception throughout the visual field. *Vision Research, 37*(15), 2073–2081, http://www.sciencedirect.com/science/article/pii/S0042698997000126.

Birch, J., Barbur, J. L., & Harlow, A. J. (1992). New method based on random luminance masking for

measuring isochromatic zones using high resolution colour displays. *Ophthalmic and Physiological Optics, 12*(2), 133–136, http://dx.doi.org/10.1111/j.1475-1313.1992.tb00275.x.

Bompas, A., Sterling, T., Rafal, R. D., & Sumner, P. (2008). Naso-temporal asymmetry for signals invisible to the retinotectal pathway. *Journal of Neurophysiology, 100*(1), 412–421, http://jn.physiology.org/cgi/content/abstract/100/1/412, doi:10.1152/jn.90312.2008.

Bompas, A., & Sumner, P. (2008). Sensory sluggishness dissociates saccadic, manual, and perceptual responses: An S-cone study. *Journal of Vision, 8*(8):10, 1–13, http://journalofvision.org/content/8/8/10, doi:10.1167/8.8.10. [PubMed] [Article]

Bowmaker, J. K., & Dartnall, H. J. (1980). Visual pigments of rods and cones in a human retina. *The Journal of Physiology, 298*(1), 501–511, http://jphysiol.highwire.org/content/298/1/501.abstract.

Bowmaker, J. K., Dartnall, H. J., Lythgoe, J. N., & Mollon, J. D. (1978). The visual pigments of rods and cones in the rhesus monkey, Macaca mulatta. *The Journal of Physiology, 274*(1), 329–348, http://jphysiol.highwire.org/content/274/1/329.abstract.

Bumsted, K., & Hendrickson, A. (1999). Distribution and development of short-wavelength cones differ between Macaca monkey and human fovea. *The Journal of Comparative Neurology, 403*(4), 502–516.

Calkins, D. J. (2001). Seeing with S cones. *Progress in Retinal and Eye Research*, *20*(3), 255–287, http://www.sciencedirect.com/science/article/pii/S1350946200000264.

Cavanagh, P., MacLeod, D. I. A., & Anstis, S. M. (1987). Equiluminance: Spatial and temporal factors and the contribution of blue-sensitive cones. *Journal of the Optical Society of America A, 4*(8), 1428–1438.

Curcio, C. A., Sloan, K. R., Packer, O., Hendrickson, A. E., & Kalina, R. E. (1987). Distribution of cones in human and monkey retina: Individual variability and radial asymmetry. *Science, 236*(4801), 579–582, http://www.sciencemag.org/content/236/4801/579.abstract, doi:10.1126/science.3576186.

Dacey, D. M. (2004). Origins of perception: Retinal ganglion cell diversity and the creation of parallel visual pathways. In M. Gazzaniga (Ed.), *The cognitive neurosciences* (pp. 281–301). Cambridge, MA: MIT Press.

Dacey, D. M., & Lee, B. B. (1994). The 'blue-on' opponent pathway in primate retina originates from a distinct bistratified ganglion cell type. *Nature, 367*(6465), 731–735, http://dx.doi.org/10.1038/367731a0.

Dacey, D. M., Liao, H.-W., Peterson, B. B., Robinson, F. R., Smith, V. C., Pokorny, J., et al. (2005). Melanopsin-expressing ganglion cells in primate retina signal colour and irradiance and project to the LGN. *Nature, 433*(7027), 749–754, http://dx.doi.org/10.1038/nature03387.

de Monasterio, F. M. (1978). Properties of ganglion cells with atypical receptive-field organization in retina of macaques. *Journal of Neurophysiology, 41*(6), 1435–1449, http://jn.physiology.org/cgi/content/abstract/41/6/1435.

De Valois, R. L., Morgan, H. C., Polson, M. C., Mead, W. R., & Hull, E. M. (1974). Psychophysical studies of monkey vision–I. Macaque luminosity and color vision tests. *Vision Research, 14*(1), 53–67, http://www.sciencedirect.com/science/article/B6T0W-484DWJB-GT/2/b96837f561fcbf7866c6350eaf6b9241.

Derrington, A. M., Krauskopf, J., & Lennie, P. (1984). Chromatic mechanisms in lateral geniculate nucleus of macaque. *The Journal of Physiology, 357*(1), 241–265, http://jphysiol.highwire.org/content/357/1/241.abstract.

Eisner, A., & MacLeod, D. I. A. (1980). Blue-sensitive cones do not contribute to luminance. *Journal of the Optical Society of America, 70*(1), 121–123.

Field, G. D., Gauthier, J. L., Sher, A., Greschner, M., Machado, T. A., Jepson, L. H., et al. (2010). Functional connectivity in the retina at the resolution of photoreceptors. *Nature, 467*(7316), 673–677, http://dx.doi.org/10.1038/nature09424, http://www.nature.com/nature/journal/v467/n7316/abs/nature09424.html#supplementary-information.

Franke, T. M., Ho, T., & Christie, C. A. (2012). The chi square test: Often used and more often misinterpreted. *American Journal of Evaluation*, *33*(3), 448–458, http://aje.sagepub.com/content/33/3/448.

Goodman, L. A. (1964). Simultaneous confidence intervals for contrasts among multinomial populations. *The Annals of Mathematical Statistics, 35*(2), 716–725, http://www.jstor.org/stable/2238523.

Hendry, S. H. C., & Reid, R. C. (2000). The koniocellular pathway in primate vision. *Annual Reviews of Neuroscience, 23,* 127–153.

Huang, X., MacEvoy, S. P., & Paradiso, M. A. (2002). Perception of brightness and brightness illusions in the macaque monkey. *The Journal of Neuroscience, 22*(21), 9618–9625, http://www.jneurosci.org/content/22/21/9618.abstract.

Judge, S., Richmond, B., & Chu, F. (1980). Implantation of magnetic search coils for measurement of

eye position: An improved method. *Vision Research, 20*(6), 535–538.

Klug, K., Herr, S., Ngo, I. T., Sterling, P., & Schein, S. (2003). Macaque retina contains an S-Cone OFF midget pathway. *The Journal of Neuroscience, 23*(30), 9881–9887, http://www.jneurosci.org/content/23/30/9881.abstract.

Lee, B. B. (2011). Visual pathways and psychophysical channels in the primate. *Journal of Physiology*, *589*(1), 41–47.

Lee, B. B., Martin, P. R., & Valberg, A. (1988). The physiological basis of heterochromatic flicker photometry demonstrated in the ganglion cells of the macaque retina. *Journal of Physiology, 404,* 323–347.

Leh, S. E., Mullen, K. T., & Ptito, A. (2006). Absence of S-cone input in human blindsight following hemispherectomy. *European Journal of Neuroscience, 24*(10), 2954–2960, http://dx.doi.org/10.1111/j.1460-9568.2006.05178.x.

Leh, S. E., Ptito, A., Schönwiesner, M., Chakravarty, M. M., & Mullen, K. T. (2010). Blindsight mediated by an S-Cone-independent collicular pathway: An fMRI study in hemispherectomized subjects. *Journal of Cognitive Neuroscience, 22*(4), 670–682, http://www.mitpressjournals.org/doi/abs/10.1162/jocn.2009.21217, doi:10.1162/jocn.2009.21217.

Logothetis, N. K., & Charles, E. R. (1990). The minimum motion technique applied to determine isoluminance in psychophysical experiments with monkeys. *Vision Research, 30*(6), 829–838, http://www.sciencedirect.com/science/article/B6T0W-4835XGM-Y7/2/9da22b12e68ada09342577cba3015513.

MacLeod, D. I. A., & Boynton, R. M. (1979). Chromaticity diagram showing cone excitation by stimuli of equal luminance. *Journal of the Optical Society of America, 69*(8), 1183–1186, http://www.opticsinfobase.org/abstract.cfm?URI=josa-69-8-1183.

Mollon, J. D., & Polden, P. G. (1975). Colour illusion and evidence for interaction between cone mechanisms. *Nature, 258*(5534), 421–422, http://dx.doi.org/10.1038/258421a0.

Ripamonti, C., Woo, W. L., Crowther, E., & Stockman, A. (2009). The S-cone contribution to luminance depends on the M- and L-cone adaptation levels: Silent surrounds? *Journal of Vision, 9*(3): 10, 1–16, http://www.journalofvision.org/content/9/3/10, doi:10.1167/9.3.10. [PubMed] [Article]

Savazzi, S., Fabri, M., Rubboli, G., Paggi, A., Tassinari, C. A., & Marzi, C. A. (2007). Interhemispheric transfer following callosotomy in humans: Role of the superior colliculus. *Neuropsychologia, 45*(11), 2417–2427, http://www.sciencedirect.com/science/article/B6T0D-4NFH0HX-4/2/6ec6dadf85d4b3855eeb9d10fb6264da.

Savazzi, S., & Marzi, C. A. (2004). The superior colliculus subserves interhemispheric neural summation in both normals and patients with a total section or agenesis of the corpus callosum. *Neuropsychologia, 42*(12), 1608–1618, http://www.sciencedirect.com/science/article/B6T0D-4CJCSSY-2/2/ea7d5acba81d7136bab90c22db5b65d7.

Schiller, P. H., & Colby, C. L. (1983). The responses of single cells in the lateral geniculate nucleus of the rhesus monkey to color and luminance contrast. *Vision Research, 23*(12), 1631–1641, http://www.sciencedirect.com/science/article/B6T0W-484M7BP-182/2/19d75fe9ba81f3351d56fd09f34083d0.

Schiller, P. H., & Malpeli, J. G. (1978). Functional specificity of lateral geniculate nucleus laminae of the rhesus monkey. *Journal of Neurophysiology, 41*(3), 788–797, http://jn.physiology.org/content/41/3/788.abstract.

Schiller, P. H., Malpeli, J. G., & Schein, S. J. (1979). Composition of geniculostriate input ot superior colliculus of the rhesus monkey. *Journal of Neurophysiology, 42*(4), 1124–1133, http://jn.physiology.org/cgi/content/abstract/42/4/1124.

Smith, V. C., & Pokorny, J. (1975). Spectral sensitivity of the foveal cone photopigments between 400 and 500 nm. *Vision Research, 15*(2), 161–171, http://www.sciencedirect.com/science/article/pii/0042698975902035.

Smithson, H. E., & Mollon, J. D. (2004). Is the S-opponent chromatic sub-system sluggish? *Vision Research, 44*(25), 2919–2929, http://www.sciencedirect.com/science/article/B6T0W-4D7K01J-1/2/acb05c7669903ce64f5cf1653faa10cb.

Smithson, H. E., Sumner, P., & Mollon, J. D. (2003). How to find a tritan line. In J. D. Mollon, J. Pokorny, & K. Knoblauch (Eds.), *Normal and defective colour vision* (pp. 279–287). Oxford: Oxford University Press.

Snodderly, D. M., Auran, J. D., & Delori, F. C. (1984a). The macular pigment. II. Spatial distribution in primate retinas. *Investigative Ophthalmology & Visual Science, 25*(6): 674–685, http://www.iovs.org/content/25/6/674.abstract. [Abstract]

Snodderly, D. M., Brown, P. K., Delori, F. C., &

Auran, J. D. (1984b). The macular pigment. I. Absorbance spectra, localization, and discrimination from other yellow pigments in primate retinas. *Investigative Ophthalmology & Visual Science, 25*(6): 660–673, http://www.iovs.org/content/25/6/660.abstract. [Abstract]

Sumner, P., Adamjee, T., & Mollon, J. D. (2002). Signals invisible to the collicular and magnocellular pathways can capture visual attention. *Current Biology, 12*(15), 1312–1316, http://www.sciencedirect.com/science/article/B6VRT-46H835B-M/2/7a141bca6c8445f49c17277b86d3c59d.

Sumner, P., Nachev, P., Castor-Perry, S., Isenman, H., & Kennard, C. (2006). Which visual pathways cause fixation-related inhibition? *Journal of Neurophysiology, 95*(3), 1527–1536, http://jn.physiology.org/cgi/content/abstract/95/3/1527, doi:10.1152/jn.00781.2005.

Sumner, P., Nachev, P., Vora, N., Husain, M., & Kennard, C. (2004). Distinct cortical and collicular mechanisms of inhibition of return revealed with S cone stimuli. *Current Biology, 14*(24), 2259–2263, http://www.sciencedirect.com/science/article/B6VRT-4F494JR-Y/2/c920ad9cd916c2dc7456f08ed5b6ae5e.

Sun, H., Smithson, H. E., Zaidi, Q., & Lee, B. B. (2006). Specificity of cone inputs to macaque retinal ganglion cells [Abstract]. *Journal of Neurophysiology, 95*(2), 837–849, http://jn.physiology.org/content/95/2/837, doi:10.1152/jn.00714.2005.

Tailby, C., Solomon, S. G., & Lennie, P. (2008). Functional asymmetries in visual pathways carrying S-cone signals in macaque. *The Journal of Neuroscience, 28*(15), 4078–4087, http://www.jneurosci.org/content/28/15/4078.abstract, doi:10.1523/jneurosci.5338-07.2008.

Trieschmann, M., van Kuijk, F. J. G. M., Alexander, R., Hermans, P., Luthert, P., Bird, A. C., et al. (2007). Macular pigment in the human retina: Histological evaluation of localization and distribution. *Eye, 22*(1), 132–137, http://dx.doi.org/10.1038/sj.eye.6702780.

Yokoyama, S., & Yokoyama, R. (1989). Molecular evolution of human visual pigment genes. *Molecular Biology and Evolution, 6*(2), 186–197, http://mbe.oxfordjournals.org/content/6/2/186.abstract.